

PAPER

Maximum Doppler Frequency Detection Based on Likelihood Estimation With Theoretical Thresholds

Satoshi DENNO^{†a)}, *Senior Member*, Kazuma HOTTA[†], *Nonmember*, and Yafei HOU[†], *Member*

SUMMARY This paper proposes a novel maximum Doppler frequency detection technique for user moving velocity estimation. The maximum Doppler frequency is estimated in the proposed detection technique by making use of the fact that user moving velocity is not distributed continuously. The fluctuation of the channel state information during a packet is applied for the proposed detection, in which likelihood estimation is performed by comparing the fluctuation with the thresholds. The thresholds are theoretically derived on the assumption that the fluctuation is distributed with an exponential function. An approximated detection technique is proposed to simplify the theoretical threshold derivation. The performance of the proposed detection is evaluated by computer simulation. The proposed detection accomplishes better detection performance as the fluctuation values are summed over more packets. The proposed detection achieves about 90% correct detection performance in a fading channel with the $E_b/N_0 = 35$ dB, when the fluctuation values are summed over only three packets. Furthermore, the approximated detection also achieves the same detection performance.

key words: Doppler spread, the maximum Doppler Frequency, probability density function, threshold, detection blackerror rate

1. Introduction

Lots of devices around us are going to connect with the internet via wireless communications in order to improve the quality of our lives [1]. Those systems are called as internet of things (IoT). Not only devices held by users but also those attached to machines communicate with servers on the internet to collect information from those devices and to provide services based on the information. The requirements for those services depend on device environments such as devices carried by users or those attached to cars. Therefore, such device environments are necessary to detect for providing necessary services. For the purpose, many techniques have been proposed. Doppler radars and MIMO radars have been considered to detect locations and velocities of devices [2]–[4]. Wearable devices, accelerometers, and video cameras have been utilized to detect user activities [5]–[7]. Activity analysis techniques have been investigated, for instance, machine learning and support vector machines, which classify activities with information given by sensing devices such as radars and Doppler sensors [8]–[10]. Many techniques have been proposed to detect the location and trajectory of user terminals [11]–[13]. Especially, the

velocity of devices has been focused on in some literature. Most of the literature applies wireless communications for the velocity estimation [14], [15], because wireless communication functionalities are supposed to be installed on sensors for the IoT. The estimation performance has also been confirmed by the field experiments [16]. Since user activities are changing, it is desired to detect activities as fast as possible.

This paper proposes a maximum Doppler frequency detection technique for user velocity estimation. The proposed detection estimates the maximum Doppler frequency, exploiting the fact that user mobility is not continuously distributed. The fluctuation of the channel state information (CSI) during a packet is applied for the proposed maximum Doppler frequency detection. The proposed detection compares the fluctuation with the thresholds to detect the maximum Doppler frequency, which implements likelihood estimation with small complexity. The thresholds are derived on assumption that the probability density function of the fluctuation is distributed with an exponential function. We also propose an approximated theoretical threshold derivation technique, which simplifies the derivation of the theoretical thresholds. If we detect the maximum Doppler frequency, the user moving velocity can be estimated based on the relationship between the user velocity and the maximum Doppler frequency. The proposed detection carries out the CSI estimation to obtain the channel fluctuation during a packet length, and compares the fluctuation with the theoretical thresholds. Because the thresholds can be obtained in off-line calculation, the proposed detection can be implemented with small computational complexity*. We show that the proposed detection achieves superior detection performance even with a few packets.

Next section introduces a system model, and the proposed detection is explained in Sect. 3. Section 4 evaluates the performance of the detection, and concluding remarks are finally presented in Sect. 5.

Throughout the paper, $E[\zeta]$ and c^* represent the ensemble average of a variable ζ and complex conjugate of a complex number c .

2. System Model

We assume that a user terminal with an antenna moves at a

*Computational complexity is defined as the amount of on-line calculation in this paper. In other words, off-line calculation is not counted in computational complexity.

Manuscript received May 9, 2021.

Manuscript revised August 22, 2021.

Manuscript publicized October 25, 2021.

[†]The authors are with Graduate School of Natural Science and Technology, Okayama University, Okayama-shi, 700-8530 Japan.

a) E-mail: denno@okayama-u.ac.jp

DOI: 10.1587/transcom.2021EBP3075

constant speed around an access point with an antenna. The terminal sends packets to the access point to start association with the access point. L_c pilot signals are attached at the beginning and the end of the packet for channel estimation, which sandwich information signals[†]. In a word, $2L_c$ pilot signals are included in the packet. The access point estimates the CSI with the received packet to detect the information signals. In addition, the access point estimates the velocity of the terminal with a proposed technique described in the following section.

When a transmitter moves while sending signals, the signals are frequency-shifted by the Doppler frequency. The Doppler frequency is spread in mobile communication environment, even when the velocity of the transmitter is constant [17]. The maximum value of the Doppler frequency is called as the maximum Doppler frequency f_D , which is defined as $f_D = \frac{v}{c} f_{RF}$ where v , c and f_{RF} denote velocity of the user terminal, that of the electromagnetic wave, and carrier frequency of the electromagnetic wave. If the maximum Doppler frequency is estimated, the velocity of the terminal can be estimated. However, since every packet is affected by different Doppler frequency, the maximum Doppler frequency can not be estimated with a single packet in principle.

On the other hand, user moving velocity is not always continuously distributed. For instance, a user walking velocity is about 5 km/h, while a user runs at the speed of about 10 km/h. If such user activities are taken into account, it is enough to select a velocity out of candidate velocities, such as 0 km/h and 5 km/h. Next section proposes a maximum Doppler frequency detection technique with only a few packets, which can be implemented with small computational complexity.

3. Maximum Doppler Frequency Detection

3.1 Principle of Detection

We assume that velocity of a user terminal varies discretely, for instance, v_1 and v_2 ; v_1 is bigger than v_2 , i.e., $v_1 > v_2$. As the user moving velocity gets higher, i.e., v_1 , higher Doppler frequency is expected to be measured from the packets received at the access point, even if the Doppler frequency is spread. The proposed technique evaluates the fluctuation to detect the Doppler frequency as follows. Since the pilot signals are attached at the beginning and the end of a packet, our proposed technique first carries out the CSI estimation at the beginning and the end of the packet. A metric defined in the following section is evaluated that is in proportion to the fluctuation. Because we can expect that the CSI is fluctuating dynamically in a packet as the Doppler frequency gets higher, if the metric is bigger than the threshold, we conclude that the terminal moves at the velocity v_1 . Otherwise, the terminal velocity is decided to be v_2 . As is described

[†]Since we assume that the proposed technique explained in Sect. 3 is applied to the advertising mode packets of the Bluetooth low energy (BLE), single carrier modulation is used.

above, the threshold plays an important role in our proposed detection technique, which is derived in the following section.

Let $\bar{h}_0(k) \in \mathbb{C}$ and $\bar{h}_{N-1}(k) \in \mathbb{C}$ denote estimated CSIs at the beginning and the end of the k th packet respectively, where N represents the number of the information signals sandwiched by the pilot signals at the beginning and the end of the packet, we define an instantaneous metric expected to be proportional to the fluctuation as follows.

$$\epsilon(k) = |\bar{h}_{N-1}(k) - \bar{h}_0(k)|^2 \quad (1)$$

In the above equation, $\epsilon(k) \in \mathbb{R}$ indicates the instantaneous metric of the k th packet. Let $h_0(k) \in \mathbb{C}$ and $h_{N-1}(k) \in \mathbb{C}$ represent CSIs at the beginning and the end of the k th packet, when the least-squares estimation [18] is applied for the channel estimation, the ensemble average of the instantaneous metric can be derived as follows.

$$\begin{aligned} \mathbb{E}[\epsilon(k)] &= \mathbb{E}\left[|\bar{h}_{N-1}(k) - \bar{h}_0(k)|^2\right] \\ &= 2\mathbb{E}\left[|\bar{h}_0(k) - h_0(k)|^2\right] \\ &\quad + 2\left(\mathbb{E}\left[|h_0(k)|^2\right] - \mathbb{E}\left[\Re\left[h_0(k)h_{N-1}^*(k)\right]\right]\right) \\ &= 2\sigma_c^2 + 2(1 - J_0(2\pi f_D T(N-1))) \end{aligned} \quad (2)$$

In (2), $J_0(x) \in \mathbb{R}$ and $\sigma_c^2 \in \mathbb{R}$ indicate the Bessel function of the first kind and the ensemble average of the channel estimation error defined as $\sigma_c^2 = \mathbb{E}\left[|\bar{h}_m(k) - h_m(k)|^2\right] = \frac{2\sigma^2}{L_c}$ where $2\sigma^2 \in \mathbb{R}$ and $m \in \mathbb{N}$ denote the AWGN power and a time index ranging from 0 to $N-1$, i.e., $0 \leq m \leq N-1$.

3.2 Probability Density Function of Channel Fluctuation

As is described in (2), the maximum Doppler frequency f_D is included in the Bessel function, while the other term in the right hand is a function of the AWGN power. In a word, the metric consists of terms caused by the maximum Doppler frequency and the AWGN. This means that the instantaneous metric $\epsilon(k)$ can be decomposed into two parts, i.e., $\epsilon_c(k) \in \mathbb{R}$ and $\epsilon_d(k) \in \mathbb{R}$, which represent a channel deviation caused by the AWGN and a fluctuation value caused by the Doppler frequency.

$$\epsilon(k) = \epsilon_c(k) + \epsilon_d(k) \quad (3)$$

Because the AWGN is distributed with the Gaussian distribution, the probability density function (PDF) of the deviation $\epsilon_c(k)$ can be written by an exponential function. As is described above, the channel fluctuation in a packet is different packet by packet, even if the maximum Doppler frequency is constant. If we assume that the channel fluctuation varies randomly just like Gaussian random variables, the fluctuation $\epsilon_d(k)$ will be distributed with an exponential function. Let $P_{PDF}(\epsilon_c) \in \mathbb{R}$ and $P_{PDF}(\epsilon_d) \in \mathbb{R}$ indicate PDFs of $\epsilon_c(k)$ and $\epsilon_d(k)$, those functions can be expressed as,

$$P_{PDF}(\epsilon_c) = k_c e^{-k_c \epsilon_c}, \quad (4)$$

$$P_{\text{PDF}}(\epsilon_d) = k_d e^{-k_d \epsilon_d}. \quad (5)$$

$k_c \in \mathbb{R}$ in (4) and $k_d \in \mathbb{R}$ in (5) represent a reciprocal of the mean value of the deviation $\epsilon_c(k)$ and that of $\epsilon_d(k)$. If (2) is taken into account, they can be defined as follows.

$$\frac{1}{k_c} = 2\sigma_c^2 \quad (6)$$

$$\frac{1}{k_d} = 2(1 - J_0(2\pi f_D T(N-1))) \quad (7)$$

Since the metric is a sum of the deviation value and the fluctuation value as shown in (3), the PDF of the metric, $P_{\text{PDF}}(\epsilon) \in \mathbb{R}$, can be expressed as,

$$P_{\text{PDF}}(\epsilon) = \frac{k_c k_d}{k_d - k_c} (e^{-k_c \epsilon} - e^{-k_d \epsilon}), \quad k_c \neq k_d. \quad (8)$$

The PDF $P_{\text{PDF}}(\epsilon)$ also consists of the two exponential functions.

3.3 Theoretical Thresholds

As is described above, when the terminal moves at the velocity v_1 or v_2 , the maximum Doppler frequency of the received signal spectrum becomes $f_{D_1} = \frac{v_1}{c} f_{\text{RF}}$ or $f_{D_2} = \frac{v_2}{c} f_{\text{RF}}$, respectively. The PDFs of the metrics for the two velocities are expressed as,

$$P_{\text{PDF}}^{(v_1)}(\epsilon) = \frac{k_c k_{d_1}}{k_{d_1} - k_c} (e^{-k_c \epsilon} - e^{-k_{d_1} \epsilon}), \quad (9)$$

$$P_{\text{PDF}}^{(v_2)}(\epsilon) = \frac{k_c k_{d_2}}{k_{d_2} - k_c} (e^{-k_c \epsilon} - e^{-k_{d_2} \epsilon}). \quad (10)$$

In the above equations, $P_{\text{PDF}}^{(v_1)}(\epsilon)$ and $P_{\text{PDF}}^{(v_2)}(\epsilon)$ indicate PDFs of the metric when the terminal moves at the velocity of v_1 and v_2 , respectively, where k_{d_i} , $i = 1$ or 2 represents a reciprocal of the ensemble average of the fluctuation value. The reciprocal of the ensemble average k_{d_i} , $i = 1$ or 2 is defined as,

$$\frac{1}{k_{d_1}} = 2(1 - J_0(2\pi f_{D_1} T(N-1))), \quad (11)$$

$$\frac{1}{k_{d_2}} = 2(1 - J_0(2\pi f_{D_2} T(N-1))). \quad (12)$$

When the PDFs for the two maximum Doppler frequencies are defined, the cumulative density function (CDF) and the complementary cumulative density function (CCDF) can be easily calculated based on the following formulae.

$$P_{\text{CDF}}^{(v_i)}(\epsilon) = \int_0^\epsilon P_{\text{PDF}}^{(v_i)}(t) dt, \quad P_{\text{CCDF}}^{(v_i)}(\epsilon) = \int_\epsilon^\infty P_{\text{PDF}}^{(v_i)}(t) dt \quad (13)$$

Let ϵ_0 represent the threshold, when the terminal moves at the velocity v_2 , for instance, the detection error rate can be expressed as $P_{\text{CCDF}}^{(v_2)}(\epsilon_0)^\dagger$. On the other hand, when the termi-

[†]The detection error rate is defined as a probability that the velocity v_1 is detected, even if the velocity of the terminal is v_2 . On the other hand, since most conventional velocity estimation techniques estimate the velocity \bar{v}_2 , the performance is evaluated by the detection error $\delta v_2 = |v_2 - \bar{v}_2|$. Therefore, the detection performance of the proposed technique can not be easily compared with conventional techniques.

nal velocity is v_1 , the detection error rate can be defined as $P_{\text{CCDF}}^{(v_1)}(\epsilon_0)$. As the threshold ϵ_0 is set to a smaller value, the detection error rate $P_{\text{CDF}}^{(v_2)}(\epsilon_0)$ is reduced, while the detection error rate $P_{\text{CCDF}}^{(v_1)}(\epsilon_0)$ gets worse. There is a trade-off between the two detection error rate performances with respect to the threshold. This means that there is the optimum threshold, which can be defined as,

$$P_{\text{CCDF}}^{(v_1)}(\epsilon_0) = P_{\text{CDF}}^{(v_2)}(\epsilon_0). \quad (14)$$

When the PDF is defined in (8), the CDF $P_{\text{CDF}}^{(v_i)}(\epsilon)$ is a monotonically increasing function with respect to ϵ , while the CCDF $P_{\text{CCDF}}^{(v_i)}(\epsilon)$ is a monotonically decreasing function. Therefore, the optimum threshold exists uniquely. The theoretical detection error rate is defined as $P_{\text{CCDF}}^{(v_1)}(\epsilon_0)$.

3.4 Channel Fluctuation Aggregation

When a PDF $P(x)$ is defined as an exponential function, its CDF is increasing gradually as x increases. Because the functions $P_{\text{PDF}}^{(v_1)}(\epsilon)$ and $P_{\text{PDF}}^{(v_2)}(\epsilon)$ are expressed with exponential functions, the theoretical detection error rate performance $P_{\text{CCDF}}^{(v_1)}(\epsilon_0)$ can not be reduced enough when the maximum Doppler frequency f_{D_2} is close to f_{D_1} . To improve the theoretical detection performance, we propose to apply multiple packets for the metric generation, which is expected to get $P_{\text{CDF}}^{(v_i)}(\epsilon)$ steep with respect to ϵ .

Let M denote the number of the packets used for the metric generation, an instantaneous metric $\epsilon_M(k) \in \mathbb{R}$ made from the M packets can be defined as,

$$\begin{aligned} \epsilon_M(k) &= \sum_{m=0}^{M-1} \left| \bar{h}_{N-m}(k-i) - \bar{h}_0(k-m) \right|^2 \\ &= \sum_{m=0}^{M-1} \epsilon(k-m) \end{aligned} \quad (15)$$

Even if the consecutive M packets are applied, the correlation of the metric $\epsilon(k-m)$ between the two packets is expected to be small because there is usually some packet interval between two packets. If the correlation is neglected, the PDF of the metric $\epsilon_M \in \mathbb{R}$ can be obtained with the famous formula as follows.

$$P_{\text{PDF}}^{(v_i)}(\epsilon_M) = \int_0^\infty \dots \int_0^{P_{(1)}^{(M-2)}} \prod_{n=1}^{M-1} P_{\text{PDF}}^{(v_i)}(\epsilon_n) P_{\text{PDF}}^{(v_i)}\left(\epsilon_M - \sum_{i=1}^{M-1} \epsilon_i\right) \prod_{n=1}^{M-1} d\epsilon_n, \quad (16)$$

where $p_{(1)}^{(M-2)} \in \mathbb{R}$ is defined as $p_{(1)}^{(M-2)} = \epsilon_M - \sum_{i=1}^{M-2} \epsilon_i$.

Because the PDF defined in (8) consists of the two exponential functions, the mathematical expression of the PDF $P_{\text{PDF}}^{(v_i)}(\epsilon_M)$ gets more complex as the number of the packets M increases. We shows some examples as follows.

- $M = 2$

$$P_{\text{PDF}}^{(v_i)}(\epsilon_2) = \left(\frac{k_{d_i} k_c}{k_{d_i} - k_c} \right)^2 \left\{ \left(\epsilon_2 - \frac{2}{k_{d_i} - k_c} \right) e^{-k_c \epsilon_2} \right.$$

$$- \left(\epsilon_2 + \frac{2}{k_{d_i} - k_c} \right) e^{-k_{d_i} \epsilon_2} \Big\} \quad i = 1, 2 \quad (17)$$

- $M = 3$

$$\begin{aligned} P_{\text{PDF}}^{(v_i)}(\epsilon_3) &= \left(\frac{k_{d_i} k_c}{k_{d_i} - k_c} \right)^3 \\ &\bullet \left[\left\{ \frac{\epsilon_3^2}{2} - \frac{3\epsilon_3}{k_{d_i} - k_c} + \frac{6}{(k_{d_i} - k_c)^2} \right\} e^{-k_c \epsilon_3} \right. \\ &\quad \left. - \left\{ \frac{\epsilon_3^2}{2} + \frac{3\epsilon_3}{k_{d_i} - k_c} + \frac{6}{(k_{d_i} - k_c)^2} \right\} e^{-k_{d_i} \epsilon_3} \right] \\ &\quad i = 1, 2 \quad (18) \end{aligned}$$

The PDF $P_{\text{PDF}}^{(v_i)}(\epsilon_M)$ comprises some component functions in the form of the exponential functions multiplied with less than M th power of ϵ_M . The CDF $P_{\text{CDF}}^{(v_i)}(\epsilon_M)$ also consists of the linear combination of those component functions.

Some mathematical manipulation is necessary to obtain the PDF $P_{\text{PDF}}^{(v_i)}(\epsilon_M)$. The following section proposes a technique to simply obtain the PDF $P_{\text{PDF}}^{(v_i)}(\epsilon_M)$.

3.5 Noise Ensemble Average Approximation

As is described in (3), the metric $\epsilon(k)$ consists of the channel fluctuation $\epsilon_d(k)$ and the deviation $\epsilon_c(k)$. While the fluctuation is greatly dependent on the maximum Doppler frequency and changes packet by packet, the deviation is distributed with the Gaussian distribution in every packet. We propose to replace the deviation $\epsilon_c(k)$ with its mean value.

$$\begin{aligned} \epsilon_M(k) &= \sum_{m=0}^{M-1} (\epsilon_d(k-m) + \epsilon_c(k-m)) \\ &\approx \sum_{m=0}^{M-1} \epsilon_d(k-m) + 2M\sigma_c^2 \end{aligned} \quad (19)$$

In the above approximation, $\epsilon_c(k)$ is replaced with $2\sigma_c^2$ in (19). Because the term $2\sigma_c^2$ is constant, the approximated PDF can be easily derived based on (16) for any number of the packet M as follows.

$$P_{\text{PDF}}^{(v_i)}(\epsilon_M) = \begin{cases} k_{d_i}^M \frac{(\epsilon_M - 2M\sigma_c^2)^{M-1}}{(M-1)!} e^{-k_{d_i}(\epsilon_M - 2M\sigma_c^2)} & \epsilon_M > 2M\sigma_c^2 \\ 0 & \epsilon_M \leq 2M\sigma_c^2 \end{cases} \quad (20)$$

As is shown in (20), the approximated PDF is reduced to the Chi-square distribution. We can easily obtain the CDF and the CCDF based on the formulae in (13) in spite of the number of the packets M , because the CCDF and the CDF of a Chi-square distribution are well-known. The easy calculation of the CCDF and the CDF reduces the effort to derive the theoretical thresholds[†].

[†]The CDF and the CCDF of a Chi-square distribution are easy to derive, while those of the PDF defined in (16) are a little bit more difficult to derive as the number of the aggregation packets M increases. Because the CDF and the CCDF are necessary to calculate the theoretical thresholds, the proposed approximation can relieve system developers from the difficult off-line calculation. This is the benefit of the proposed ensemble average approximation.

Table 1 Simulation parameters.

Modulation	BPSK/Single Carrier
No. of antennas on terminal	1
No. of antennas on access point	1
Channel model	Rayleigh fading
Channel estimation	Least-squares estimation
Velocity of terminal	0 km/h, 5 km/h, 10 km/h
RF frequency	2.4 GHz
Symbol rate	1 MHz
The number of information signals in a packet	120
The number of pilot symbols L_c	30

4. Simulation

The performance of the proposed detection is verified by computer simulation. The binary phase shift keying (BPSK) modulation is applied. The number of antennas on a terminal and an access point is only 1 as described above. The least-squares estimation is applied for the channel estimation [18] as is described above. The channel between the terminal and the access point is modeled with Rayleigh fading based on Jakes' model [17]. Carrier frequency f_{RF} and symbol rate $1/T$ are 2.4 GHz and 1 MHz, respectively. Two scenarios are utilized for the performance evaluation. In one scenario, the terminal velocity is switched back and forth between 0 km/h and 5 km/h with equal probability, packet by packet. The terminal velocity is changed between 5 km/h and 10 km/h with equal probability, packet by packet in the other scenario. The simulation parameters are summarized in Table 1.

4.1 Cumulative Distribution Functions

Before the performance evaluation of the proposed detection, the PDF theoretically derived above is compared with that obtained by the computer simulation. Figure 1 shows the comparison in the first scenario, i.e., $v_1 = 5$ km/h, $v_2 = 0$ km/h. In the figure, the solid line and the dotted line represent the theoretical PDF and the PDF obtained by the computer simulation, respectively. The abscissa is the metric ϵ_3 , and the right ordinate and the left ordinate are the CDF and the CCDF, respectively. In the figure, the CDF $P_{\text{CDF}}^{(v_1)}(\epsilon)$ and the CCDF $P_{\text{CCDF}}^{(v_2)}(\epsilon)$ are shown. The number of the packets M is set to 3 and the $E_b/N_0 = 15$ dB. The theoretical threshold derived above is also added in the figure. The theoretical CCDF well agrees with the CCDF obtained through the computer simulation, while the CDF obtained by the computer simulation is slightly deviated from the theoretical CDF. Although the proposed detection with the theoretical thresholds is expected to achieve the best detection performance, the detection error rate is about 0.5.

Figure 2 shows the comparison in the first scenario with the $E_b/N_0 = 35$ dB. The other parameters are the same to those of Fig. 1. While the theoretical CCDF well agrees with that obtained by the computer simulation, the theoretical commutative distribution function $P_{\text{CDF}}^{(v_1)}(\epsilon)$ is a little bit

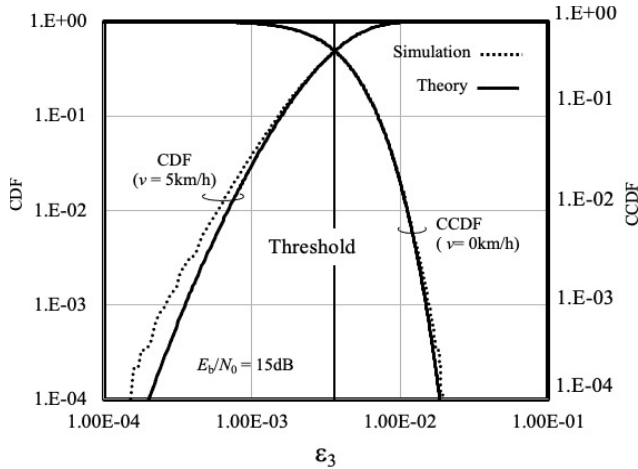


Fig. 1 Cumulative density functions at $E_b/N_0 = 15$ dB with $M = 3$.

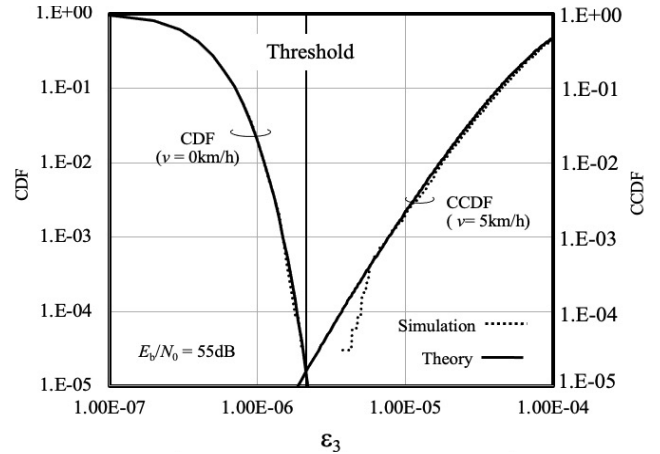


Fig. 3 Cumulative density functions at $E_b/N_0 = 55$ dB with $M = 3$.

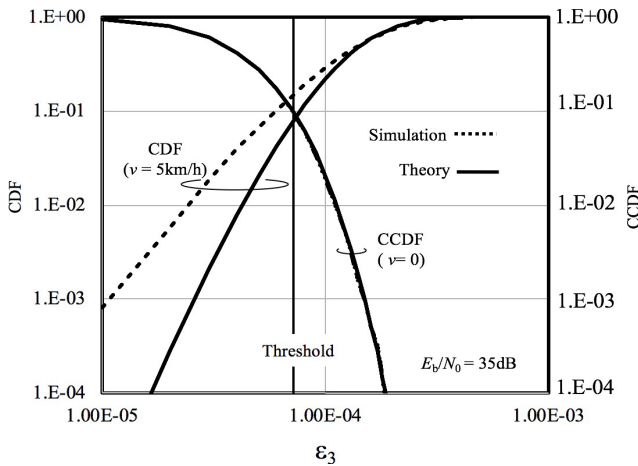


Fig. 2 Cumulative density functions at $E_b/N_0 = 35$ dB with $M = 3$.

different from the function obtained by the computer simulation.

This performance gap is caused by the correlation between the deviation $\epsilon_c(k)$ and the fluctuation $\epsilon_d(k)$. Although the correlation is assumed to be zero in the theoretical derivation described previously, actually, they are made correlated with each other in the CSI estimation. On the other hand, since the theoretical CCDF is derived without the channel fluctuation, there is no correlation in principle. This is the reason why the theoretical CCDF well agrees with the CCDF obtained by the computer simulation. Consequently, because the correlation is not taken into account in the theoretical CDF derivation, the theoretical CDF is a little bit different from the CDF obtained by the computer simulation.

Figure 3 shows the comparison in the first scenario with the $E_b/N_0 = 55$ dB. The other parameters are the same to those of Fig. 1. The theoretical performances well agrees with the performances obtained through the computer simulation. Since the AWGN is negligibly small, the correlation between the deviation and the fluctuation can be negligibly

small. The CDF is dominated by that of the fluctuation. Therefore, the theoretical CDF well agrees with the CDF obtained by the computer simulation.

4.2 Detection Performance

The detection error rate performance of the proposed detection is shown in Fig. 4. The first scenario is applied in the figure, i.e., $v_1 = 5$ km/h and $v_2 = 0$ km/h. The abscissa and the ordinate are the number of the packets M and the average detection error rate, respectively. The detection performances in the channel with the $E_b/N_0 = 15$ dB, 35 dB and 55 dB are drawn in the figure. As the number of the packets M increases, the detection error rate performance is improved in the channel with the $E_b/N_0 = 35$ dB and 55 dB, although the detection error rate performance is kept same despite of the number of the packets M in the channel with the $E_b/N_0 = 15$ dB[†]. The detection error rate is reduced to less than 10^{-3} when the $E_b/N_0 = 55$ dB if the number of the packets is more than 2.

Figure 5 shows the detection error rate performance in the second scenario, i.e., $v_1 = 10$ km/h and $v_2 = 5$ km/h. The abscissa and the ordinate are the number of the packets M and the average detection error rate, respectively. Although the detection error rate is kept constant in spite of the number of the packets M when the $E_b/N_0 = 15$ dB, the detection error rate performance is improved as the number of the packets M is incremented in the channel with the $E_b/N_0 = 35$ dB and 55 dB. However, the detection error rate performance in the second scenario is worse than that in the

[†]Figures 1, 2 and 3 suggest that the CDF at the threshold ϵ_0 tends to get high as the E_b/N_0 is decreased. As is shown in Fig. 1, in particular, the CDF at threshold ϵ_0 is approximately 0.5, which degrades the detection error rate to about 0.5, when the E_b/N_0 is 15 dB. As long as the E_b/N_0 is 15 dB, the CDF performance is not improved even if the number of the packets increases. When the CDF performance is the same, in principle, the proposed technique achieves the same detection performance. This is the reason why the detection performance is not improved even if the number of the packets increases.

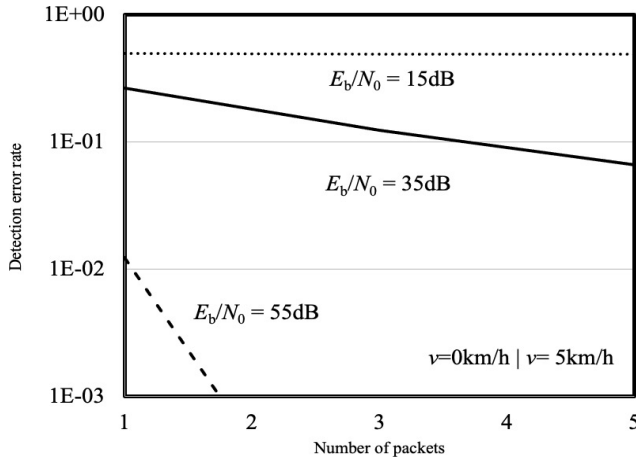


Fig. 4 Detection error rate performance v.s. number of packets ($v_2 = 0$ km/h | $v_1 = 5$ km/h).

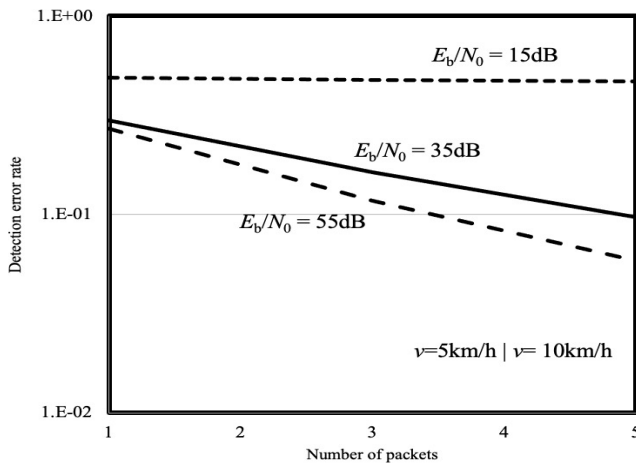


Fig. 5 Detection error rate performance v.s. number of packets ($v_2 = 5$ km | $v_1 = 10$ km/h).

first scenario. The detection performance is improved as the number of the packets M increases in spite of the scenario when the E_b/N_0 is not less than 35 dB. In a word, the proposed detection achieves higher detection performance in the channel with higher E_b/N_0 .

Figure 4 and Fig.5 show that the proposed technique can distinguish the velocities 0 km/h and 5 km/h, and 5 km/h and 10 km/h, respectively. This means that the proposed technique can distinguish 3 velocities such as 0 km/h, 5 km/h and 10 km/h with the two theoretical thresholds used in the Figs.4 and 5. Let $\epsilon_{M,0}(n)$ denote a threshold for detecting the velocities v_n and v_{n+1} , the velocities v_m $m = 1 \cdots n + 1$ can be detected if theoretical thresholds $\epsilon_{M,0}(m)$ $m = 1 \cdots n$ are obtained based on the techniques described in Sect. 3.

4.3 Noise Ensemble Average Approximation

Since the channel deviation variables are replaced with their ensemble average in the noise ensemble average approxi-

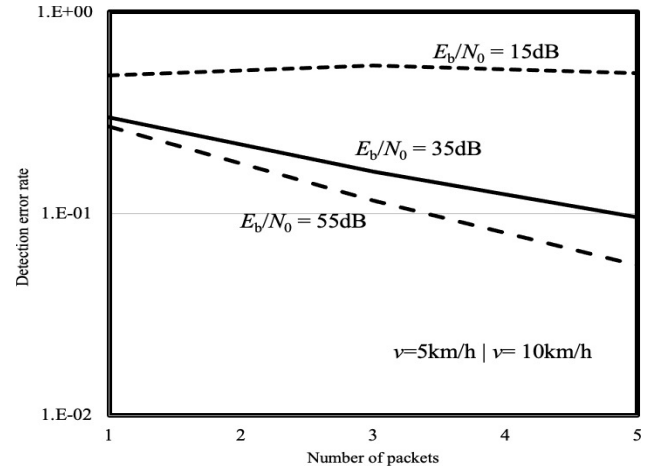


Fig. 6 Detection error rate performance of noise ensemble average approximation ($v_2 = 5$ km | $v_1 = 10$ km/h).

mation, the slope of the CDF or the CCDF depends on the distribution of the fluctuation ϵ_d . The theoretical PDF is not useful when the velocity is zero, because the fluctuation is reduced to zero in the derivation of the theoretical PDF. Therefore, the noise ensemble average approximation can not be applied to detect the Doppler frequency in the first scenario, because the velocity v_2 is 0 km/h in the first scenario. Figure 6 shows the detection error rate performance of the noise ensemble average approximation in the second scenario, i.e., $v_1 = 10$ km/h and $v_2 = 5$ km/h. Though the instantaneous deviation ϵ_c is replaced with its ensemble average in the approximation, as is shown in the figure, the proposed approximation achieves almost the same detection performance to the proposed detection shown in Fig. 5.

5. Conclusion

This paper has proposed a maximum Doppler frequency detection technique for user mobility estimation. The proposed detection estimates the maximum Doppler frequency, exploiting the fact that user mobility is not continuously distributed. The fluctuation of the channel state information during a packet is applied for the proposed maximum Doppler frequency detection based on the likelihood estimation. The proposed detection detects a Doppler frequency from discretely distributed Doppler frequency candidates based on likelihood estimation, assuming that user moving velocity is discretely distributed. The CSI fluctuation during a packet is verified and is compared with the theoretical thresholds in the proposed detection, which is regarded as a simple implementation of likelihood estimation. This paper derives the theoretical thresholds on assumption that the fluctuation is distributed with an exponential function. Furthermore, this paper proposes a noise ensemble average approximation to simplify the theoretical threshold derivation, in which the instantaneous CSI estimation errors caused by the AWGN are replaced with its ensemble average. Because the thresholds can be obtained in off-line calculation, the

proposed detection can be implemented with small computational complexity.

The performance of the proposed detection is evaluated by computer simulation. The proposed detection achieves better performance as the E_b/N_0 increases. The detection performance is also improved as more packets are applied to calculate the fluctuation in the detection. When the user mobility is switched back and forth between staying at a same place and moving at the velocity of 5 km/h, the proposed detection achieves more than 90 percent successful detection performance with only three packets as long as the E_b/N_0 is not less than 35 dB. The approximation technique achieves the same classification performance.

Summarizing, the proposed techniques attain such superior performance within very short time period, such as time length required to receive 3 packets, even though the proposed techniques can be implemented with small computational complexity.

Acknowledgments

This work was supported by NTT DOCOMO, namely, Dr. T. Okada, Mr. T. Nishizaki, Mr. K. Ichikawa, and Dr. Y. Abrakawa of the communication device development department, and JSPS KAKENHI Grant Number JP21K04061.

References

- [1] T. Ohtsuki, "A smart city based on ambient intelligence," *IEICE Trans. Commun.*, vol.E100-B, no.9, pp.1547–1553, Sept. 2017.
- [2] Y. Kim and H. Ling, "Human activity classification based on micro-Doppler signatures using a support vector machine," *IEEE Trans. Geosci. Remote Sens.*, vol.47, no.5, pp.1328–1337, May 2009.
- [3] D. Sasakawa, N. Homma, T. Nakayama, and S. Iizuka, "Human activity identification by height and Doppler RCS information detected by MIMO radar," *IEICE Trans. Commun.*, vol.E102-B, no.7, pp.1270–1278, July 2019.
- [4] M. Fujiwara, M. Fujimoto, Y. Arakawa, and K. Yasumoto, "Development and evaluation of in-home activity recognition utilizing Doppler sensor," *IPSI SIG Technical Report*, pp.1–8, 2018.
- [5] Ó.D. Lara and M.A. Labrador, "A survey on human activity recognition using wearable sensors," *IEEE Commun. Surveys Tuts.*, vol.15, no.3, pp.1192–1209, third quarter, 2013.
- [6] S.O. Slim, A. Atia, M.M.A. Elfattah, and M.-S.M. Mostafa, "Survey on human activity recognition based on acceleration data," *International Journal of Advanced Computer Science and Applications*, vol.10, no.3, pp.84–98, 2019.
- [7] T. Subetha and S. Chitrakala, "A survey on human activity recognition from videos," *Proc. International Conference on Information Communication and Embedded System (ICICES 2016)*, 2016.
- [8] J. Hong and T. Ohtsuki, "State classification with array sensor using support vector machine for wireless monitoring system," *IEICE Trans. Commun.*, vol.E95-B, no.10, pp.3088–3095, Oct. 2012.
- [9] K. Yamamoto, K. Toyoda, and T. Ohtsuki, "Doppler sensor-based blink duration estimation by analysis of eyelids closing and opening behavior on spectrogram," *IEEE Access*, vol.7, pp.42726–42734, 2019.
- [10] J. Tan, Q. Zhao, X. Guo, X. Zhao, and G. Wang, "Radio tomographic imaging based on low-rank and sparse decomposition," *IEEE Access*, vol.7, pp.50223–50231, 2019.
- [11] L. Chen, I. Ahriz, and D.L. Ruyet, "AoA-aware probabilistic indoor location fingerprinting using channel state information," *IEEE Internet Things J.*, vol.7, no.11, pp.10868–10883, 2020.
- [12] F. Zafari, A. Gkelias, and K.K. Leung, "A survey of indoor localization systems and technologies," *IEEE Commun. Surveys Tuts.*, vol.21, no.3, pp.2568–2599, 2019.
- [13] Y. Zhao and N. Patwari, "Robust estimators for variance-based device-free localization and tracking," *IEEE Trans. Mobile Comput.*, vol.14, no.10, pp.2116–2129, Oct. 2015.
- [14] T. Yücek, R.M.A. Tannious, and H. Arslan, "Doppler spread estimation for wireless OFDM systems," *IEEE/Sarnoff Symposium on Advances in Wired and Wireless Communication*, April 2005.
- [15] J.-H. Do and H.-J. Choi, "A velocity estimation-based channel estimator for WCDMA forward link receiver," *IEICE Trans. Commun.*, vol.E88-B, no.11, pp.4373–4377, Nov. 2005.
- [16] S. Maiti, M. Mikami, and K. Hoshino, "Field experimental evaluation of mobile terminal velocity estimation based on Doppler spread detection for mobility control in heterogeneous cellular networks," *IEICE Trans. Commun.*, vol.E100-B, no.2, pp.252–261, Feb. 2017.
- [17] W.C. Jakes, *Microwave Mobile Communications*, IEEE Press, 1994.
- [18] S. Haykin, *Adaptive Filter Theory*, 4th ed., Prentice Hall, 2011.



Satoshi Denno received the M.E. and Ph.D. degrees from Kyoto University, Kyoto, Japan in 1988 and 2000, respectively. He joined NTT radio communications systems labs, Yokosuka, Japan, in 1988. He was seconded to ATR adaptive communications research laboratories, Kyoto, Japan in 1997. From 2000 to 2002, he worked for NTT DOCOMO, Yokosuka, Japan. In 2002, he moved to DOCOMO communications laboratories Europe GmbH, Germany. From 2004 to 2011, he worked as an associate professor at Kyoto University. Since 2011, he is a full professor at graduate school of natural science and technology, Okayama University. From the beginning of his research career, he has been engaged in the research and development of digital mobile radio communications. In particular, he has considerable interests in channel equalization, array signal processing, Space time codes, spatial multiplexing, and multimode reception. He won the Best paper award of the 19th international symposium on wireless personal multimedia communications (WPMC2016), and the outstanding paper award of the 23rd international conference on advanced communications technology (ICAT2021). He received the excellent paper award and the best paper award from the IEICE in 1995 and from the IEICE communication society in 2020, respectively.



Kazuma Hotta received the B.E. and the M.E. from Okayama University, Okayama, Japan in 2018 and 2021, respectively. His research interests are in signal processing and signal detection for wireless communications. He joined with Mitsubishi Electric Corporation in 2021.



Yafei Hou received his Ph.D. degrees from Fudan University, China and Kochi University of Technology (KUT), Japan in 2007. He was a post-doctoral research fellow at Ryukoku University, Japan from August 2007 to September 2010. He was a research scientist at Wave Engineering Laboratories, ATR Institute International, Japan from October 2010 to March 2014. He was an Assistant Professor at the Graduate School of Information Science, Nara Institute of Science and Technology, Japan from April 2014

to March 2017. He became an assistant professor at the Graduate School of Natural Science and Technology, Okayama University, Japan from April 2017. He is a guest research scientist at Wave Engineering Laboratories, ATR Institute International, Japan from October 2016. His research interests are communication systems, wireless networks, and signal processing. He received IEICE (the Institute of Electronics, Information and Communication Engineers) Communications Society Best Paper Award in 2016, 2020, and Best Tutorial Paper Award in 2017. Dr. Hou is a senior member of IEEE and member of IEICE.